AIP Advances

Geometry of electromechanically active structures in Gadolinium - doped Cerium oxides

Yuanyuan Li, Olga Kraynis, Joshua Kas, Tsu-Chien Weng, Dimosthenis Sokaras, Renee Zacharowicz, Igor Lubomirsky, and Anatoly I. Frenkel

Citation: AIP Advances **6**, 055320 (2016); doi: 10.1063/1.4952645
View online: http://dx.doi.org/10.1063/1.4952645
View Table of Contents: http://scitation.aip.org/content/aip/journal/adva/6/5?ver=pdfcov
Published by the AIP Publishing

AIP ADVANCES **6**, 055320 (2016)

Geometry of electromechanically active structures in Gadolinium - doped Cerium oxides

Yuanyuan Li,[1] Olga Kraynis,[2] Joshua Kas,[3] Tsu-Chien Weng,[4] Dimosthenis Sokaras,[4] Renee Zacharowicz,[1] Igor Lubomirsky,[2,a] and Anatoly I. Frenkel[1,a]
[1]*Physics Department, Yeshiva University, 245 Lexington Avenue, New York, New York 10016, USA*
[2]*Department of Materials and Interfaces, Weizmann Institute of Science, Rehovot 76100, Israel*
[3]*Department of Physics, University of Washington, Seattle, Washington 98195, USA*
[4]*Stanford Synchrotron Radiation Lightsource, SLAC National Accelerator Laboratory, Menlo Park, California 94025, USA*

(Received 11 February 2016; accepted 13 May 2016; published online 20 May 2016)

Local distortions from average structure are important in many functional materials, such as electrostrictors or piezoelectrics, and contain clues about their mechanism of work. However, the geometric attributes of these distortions are exceedingly difficult to measure, leading to a gap in knowledge regarding their roles in electromechanical response. This task is particularly challenging in the case of recently reported non-classical electrostriction in Cerium-Gadolinium oxides (CGO), where only a small population of Ce-O bonds that are located near oxygen ion vacancies responds to external electric field. We used high-energy resolution fluorescence detection (HERFD) technique to collect X-ray absorption spectra in CGO in situ, with and without an external electric field, coupled with theoretical modeling to characterize three-dimensional geometry of electromechanically active units. [http://dx.doi.org/10.1063/1.4952645]

The quest to rationally design electromechanical materials, i.e., those that can develop large stress or strain under external electric field, has intensified in the last decade because these materials constitute a backbone of a large number of technologies, from micro-actuators in industrial and consumer products to ultrasound transducers.[1–4] Electrostrictors, the materials exhibiting quadratic response to the electric field, are especially attractive for actuators because they develop strain under electric field but do not generate polarization under deformation. Giant electrostriction effects were recently reported in Gd doped ceria (CGO) thin films: they can generate stress greater than 500 MPa,[5] i.e., competitive with the best electromechanically active materials currently in use.[6,7] While possessing neither a large dielectric constant nor a non-centrosymmetric lattice, which are attributes of most widely investigated electrostrictors and piezoelectrics,[8–11] CGO clearly exceeds the classical electrostrictors described by Robert Newnham by at least two orders of magnitude.[12] Recently, it was reported that another material with a fluorite structure (Nb,Y-stabilized, δ-Bi_2O_3) also exhibits giant electrostriction and, similar, to CGO contains a few percent of empty oxygen lattice sites.[13] It is likely therefore that these and other similar systems belong to a previously unknown class of electrostrictors, and understanding their microscopic mechanism will be of great fundamental and practical importance.

In the previous work we showed that the X-ray absorption spectra of Ce changed under application of an electric field, but those of Gd – did not, hinting at the dominant role of Ce in electromechanical activity of CGO.[5] Differential quick Extended X-ray Absorption Fine Structure (QEXAFS)

[a]igor.lubomirsky@weizmann.ac.il; anatoly.frenkel@yu.edu

results provided more details.[14] They uncovered the existence of electroactive Ce-O bonds in the CGO. Those bonds were ca. 0.1 Å shorter than a typical Ce-O bond length of 2.3 Å in the absence of external electric field and restored their normal lengths under the field.[14] It was proposed that these electroactive bonds are associated with Ce ions located within the distorted Ce-7O-1O_v units that contain an oxygen vacancy O_v.[5,14] While important in guiding future investigations, these recent findings were indirect and the resulting model is qualitative. Indeed, no knowledge exists about the directions and magnitudes of the distortions in the Ce-7O-1O_v unit that directly affect electrostriction and are thus the local descriptors of the electromechanical activity of CGO. Without the knowledge of the geometry of the electroactive units and its dynamic changes during application of external fields, evaluation of these descriptors and, hence, design of electrostrictive materials with pre-defined properties, are complicated.

The main challenge is thus to directly detect and quantify oxygen rearrangements and the rather large associated disorder in the various local environments of Ce atoms *in-situ*. The oxygen vacancies that, presumably, induce the local disorder occupy only a few percent of the lattice sites; making the task of distinguishing between the Ce ions with and without neighboring vacancy quite daunting. Extended X-ray Absorption Fine Structure (EXAFS) can be used to characterize the average environment of each type of absorber (Ce or Gd), but EXAFS due to the nearest neighbors has no three-dimensional sensitivity, i.e., sensitive mostly to bond lengths, not bond angles. Due to the life-time broadening[15,16] and thus relative lack of features in the Ce and Gd L_3 edge X-ray Absorption Near Edge Structure (XANES) spectra, they provide very limited information for the first principle modeling of local atomic geometry. Additionally, the ensemble-average XANES and EXAFS spectra of Ce are dominated by the signals coming from "spectator" species, i.e., those undistorted CeO_8 units that are not unaffected by the electric field. Differential[17,18] and time-resolved methods[19] of EXAFS analysis showed potential towards isolating signals coming from active species only[14] but they are relatively inefficient for three-dimensional geometric characterization, *vide supra*.

In this work, we combined the high-energy resolution fluorescence detection (HERFD) technique and first principle simulations of the data in order to identify electroactive species in CGO thin films containing a mixture of active and inactive species. The reason we employed HERFD here is that it improves sensitivity of XAS to the geometry and its changes that is hampered in conventional XANES due to the life-time broadening effects. So obtained, high-resolution spectra can be directly modeled by theories and their sensitivity to the changes in local geometry is significantly improved.[20,21] Based on the theoretical simulations of the spectra of electroactive species that we extracted from the in situ XANES measurements, we narrowed down the choice of possible structural models of active species and proposed two plausible models of distortions of the local structure around Ce caused by application of external electric field.

The Ce L_3 edge HERFD XANES was performed at beamline 6-2, SSRL using Si (311) monochromator and a high-resolution x-ray emission spectrometer.[22] Energy resolution of the spectrometer was 0.7 eV in this experiment. The geometry of the setup is shown in Figure 1, and the details are given in Supplemental Material.[23] The studied films were attached to a sample holder and illuminated at 45° of incident angle using an analysis area of 150 μm by 450 μm (FWHM). The films were deposited using Magnetron Sputtering (AJA® Sputter). First a bottom electrode of 100nm Ti was deposited on an 8×40 mm Si substrate ($n^{++}\langle 100\rangle$, 275 μm thick). On top was deposited a 400nm layer of $Ce_{1-x}Gd_xO_{2-x/2}$ where x=0.05 and 0.2. The films were annealed at 400°C under nitrogen atmosphere for 4 hours in order to release deposition strain. A top electrode of 100nm Ti+Au was deposited on top of the CGO layer, using Electron-beam evaporation (Odem®). The devices were mounted on a glass microscope slide and electrodes were connected using conductive paint. The in situ measurements were conducted as follows: The sample was mounted and 6 XANES scans were taken without any applied bias, these scans were averaged and considered as "Before poling". The subsequent applied electric field was a combination of AC and DC field and defined by $V_{app} = V_{DC} + V_{AC} \cdot \cos(2\pi f t)$ [f = 10 mHz, V_{AC} = 0.75 V, V_{DC} = 0.4 V]. Scans were taken periodically until no further changes were observed in XANES spectrum, and then the last 6 scans were merged and considered "After poling". The time to reach the poled state was between 2-12 hours.

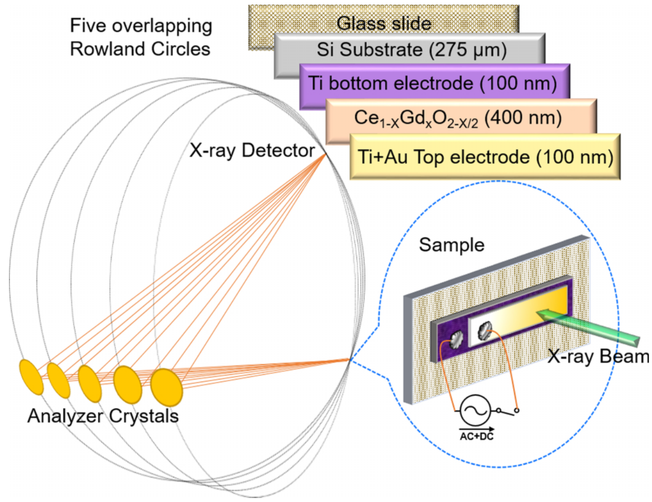

FIG. 1. Schematic of the experimental setup and layer composition of sample films.

The HERFD XANES spectra of the samples (5% and 20% Gd dopants) before and after being exposed to the electric field are shown in Figure 2(A). Compared to conventional XANES spectra which only show two major peaks in the range of 5715-5745 eV,[5,14,24,25] the HERFD spectra show five distinct resolved peaks labeled in Figure 2(A). The pre-edge peak A relates to the 2p → 4f electronic transitions and the main edge is attributed to the $2p_{3/2} \rightarrow 5d_{5/2}$ transitions.[26] Between peak A and the main edge, there is a weak peak at about 5726 eV. It is associated with the Ce^{3+} valence state[27] and attributed to a shakedown effect.[28] The change of this peak reflects the behavior of 4f valence electron.[28] The appearance of two peaks in the range of 5725-5735 eV or 5735-5745 eV is due to the crystal field splitting of 5d orbitals. Peaks B, C (assigned to screened excited states) and D, E (assigned to unscreened excited states) were found to be sensitive to the local structure around Ce.[20] For CGO films, the spectral changes before and after poling are relatively subtle but the increase in intensity of peak C after poling was observed for both films (Figure 2(A), inset), in agreement with previous differential QEXAFS experiments.[14] As emphasized above, the relatively small changes in XANES are caused by the small fraction of active species responding to the electric field.

In this work, we derived the three-dimensional structural models of distorted Ce-7O-1O_v units by simulating theoretical XANES spectra in candidate distorted structures and comparing them with experimental data. The theoretical spectra of the active species reflect only the spectral features of distorted structural units while the experimental data (Figure 2(A)) show the average spectra that

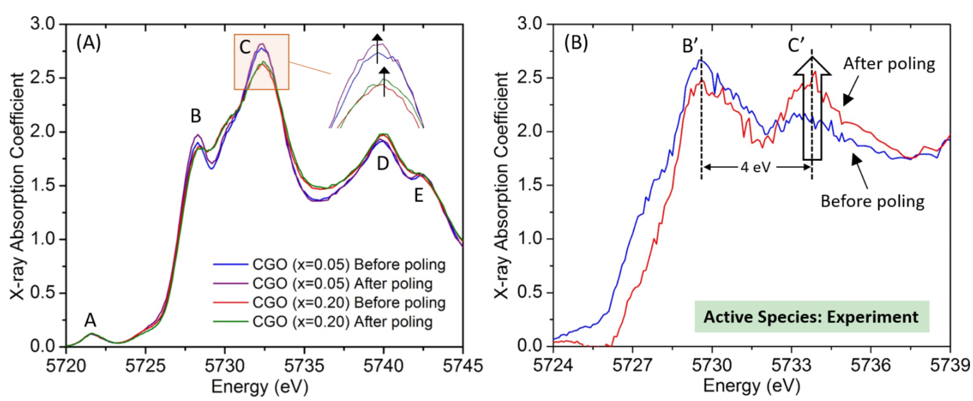

FIG. 2. (A) Normalized Ce L_3 edge XANES spectra of CGO films with Gd concentration of 0.05 and 0.20 before and after being exposed to electric field, (B) Extracted XANES spectra of electroactive species before and after poling treatment.

are dominated by the undistorted units. Therefore, before comparing experimental and theoretical XANES spectra, it is necessary to extract the XANES signals of the active species from the total experimental data. Toward that goal, we first assume that the distorted units are not strongly interacting with each other and thus the spectra of active species and spectators do not change with the concentration of Gd. We denote the experimental Ce XANES spectrum for $m\%$ and $n\%$ Gd doped CeO_2 as $D^{(m)}$ and $D^{(n)}$, respectively. Each data can then be expressed in terms of the linear combination of two spectra, Ce-8O (spectators) and Ce-7O-1O_v (active species), as follows: $D = y_s X_s + y_a X_a$ where y_s is the molar fraction of spectators and y_a is the molar fraction of active Ce atoms in the sample. From the data measured at two concentrations of Gd dopants, the unknown pure spectrum of active species, X_a, can be extracted:

$$X_a = \left(\frac{y_a^{(m)}}{y_s^{(m)}} - \frac{y_a^{(n)}}{y_s^{(n)}}\right)^{-1} \left(y_s^{(m)}\right)^{-1} D^{(m)} - \left(\frac{y_a^{(m)}}{y_s^{(m)}} - \frac{y_a^{(n)}}{y_s^{(n)}}\right)^{-1} \left(y_s^{(n)}\right)^{-1} D^{(n)} \tag{1}$$

In Eq. (1), the molar fractions for active species can be related to the concentrations of vacancies if we assume that vacancies are randomly distributed through the CGO structure. The details of these estimates are given in Supplemental Material.[23] For 5% Gd doped CeO_2, the estimates yield $y_a = 0.09$, $y_s = 0.91$ and for 20% Gd, $y_a = 0.28$, $y_s = 0.72$.

Using the XANES data for 5% and 20% Gd films and Eq. (1), the XANES spectra of the active species X_a measured before and after poling were obtained and are shown in Figure 2(B). For both spectra, there are two peaks. One is located in the range of 5729-5731 eV (peak B') and another is in the range of 5732-5737 eV (peak C'). The energy difference between these two peaks is about 4 eV. The strongest observed change in the spectrum with application of the electric field was an increase in the amplitude of the second peak (C'). This behavior is consistent with the ordering of the distorted structure of active species after poling, in agreement with the previous differential QEXAFS results where the short Ce-O bonds were found to relax to their normal lengths under electric field.[14] We constructed several plausible models in which distortions in the environment around Ce were introduced, as inputs for theoretical calculations of XANES, to compare with the behavior observed in Fig. 2(B). We focused on the strongest effect in the spectra, the change in the height of the second peak, in order to identify the candidate models. These models were further constrained by the results of our previous EXAFS study, which determined short Ce-O bonds. In Model 1 (Figure 3(A)), we shifted 6 of the 7 oxygen atoms of the active unit towards the central Ce, while shifting the one on Ce-O_v diagonal away from Ce along [111] direction. In Model 2

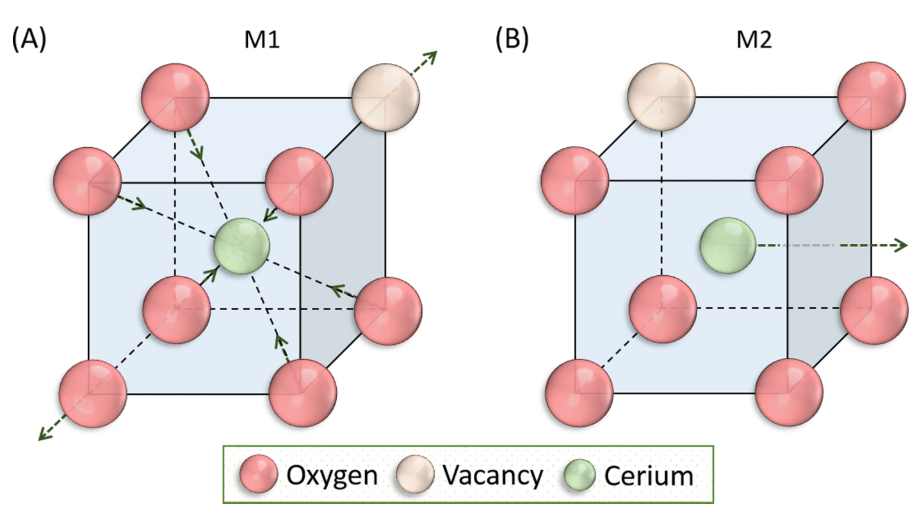

FIG. 3. The Ce-7O-1O_v models of electroactive species in CGO film. In Model 1 (A), oxygen atoms shift along [111] direction. Out of 7 nearest oxygen atoms, six of them shift towards Ce and the one diagonal to oxygen vacancy moves away from Ce. Such distortion produces 6 short Ce-O bonds and 1 long Ce-O bond. In Model 2 (B), Ce atom shifts along [010] direction, resulting in 4 short Ce-O bonds and 3 long Ce-O bonds.

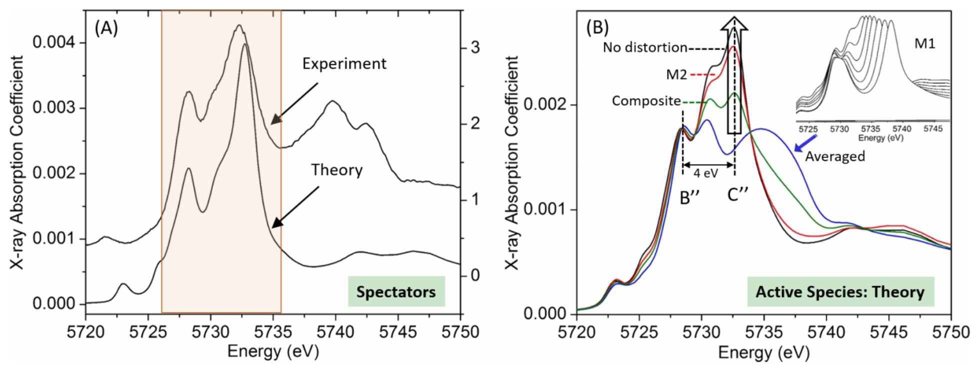

FIG. 4. (A) Comparison between simulated XANES spectrum (Theory) and isolated XANES spectrum (Experiment) for spectators (which have the local structure of Ce-8O). (B) Simulated Ce L_3 XANES spectrum of non-distorted Ce-7O-1O_v (black), Model 1 (black, inset) and Model 2 (red). For the spectra shown in Model 1 in the inset, each one was simulated by changing the O atoms positions in the direction of arrows shown in Figure 3(A), so that the value of the six Ce-O short bonds incrementally changed as follows: 2.343 (undistorted, the same spectrum as "No distortion" in figure 4) to 2.013 Å. Correspondingly, the 1 long Ce-O bond was incrementally elongated from 2.343 (undistorted) to 2.673 Å. The blue curve was produced by averaging over the seven spectra in the inset. The green spectrum corresponds to a composite model where both the distorted Model 1 and Model 2 were averaged with equal weight.

(Figure 3(B)), we shifted the central Ce along the [010] direction. Both models qualitatively agree with the total number of short bonds, estimated previously.[14] Specifically, in Model 1 there are 6 short bonds per active Ce unit, and in Model 2 there are 4 such bonds.

Based on these models, theoretical XANES spectra at the Ce L_3 edge were simulated using the FEFF9 code.[29–31] Details are presented in Supplemental Material.[23] To validate our approach, and to calibrate the quality of the simulations, we compared the simulated XANES spectrum of ideal CeO_2 and the isolated experimental XANES spectrum of spectators, X_s, whose structure should be similar to that in CeO_2 due to their lack of a vacancy near the Ce atoms. The experiment and the theory are thus expected to describe the same local units and their comparison would provide a baseline test of the theory, and guide the subsequent interpretation of the active species. The XANES spectrum of the spectators was extracted using the same method as for the active species (Eq. (1)). As shown in Figure 4(A), for both theoretical and experimental spectra, there are two distinct peaks in the same energy range of 5725-5735 eV. The position and shapes of each experimental peak are well reproduced by FEFF9, hence, they can be used for modeling the unknown structure of the active species. The peaks in the range of 5735-5750 eV are related to multiple electron processes and, therefore, could not be well simulated using the single-electron FEFF code.[26,32]

Simulations on distorted models were carried out using the same set of FEFF9 parameters as for the test described above. Similar to the experimental spectra shown in Figure 2(B), the energy difference between the two peaks (B" and C") in the range of 5725-5735 eV for simulated spectra (Figure 4(B)) is about 4 eV. Figure 4(B), inset, shows that for Model 1 (Figure 3(A)), the main effect is the shift of the peak at about 5732 eV (peak C") to the right of that in the undistorted structure (the leftmost), in disagreement with the experimental data (Figure 2(B)) where this peak decreased in intensity without an obvious shift. That decrease, however, can be obtained if we assume that the magnitudes of distortions in all units are not equal to each other (which can be explained by the random nature of the neighboring environment of the active units), but are instead distributed over a range of values. We simulated such distribution using distortions ranging from 2.013 to 2.288 Å for 6 short Ce-O bonds and 2.673 to 2.398 Å for the longer bond, and equally weighted. These values were chosen so that the previously obtained short bond length of 2.22 Å[14] fell within the distribution. Figure 4(B) shows that such averaging indeed produces the observed broadening and reduction in intensity of the main peak at ca. 5732 eV compared to the undistorted structure.

Compared to the spectrum of undistorted model (Figure 4(B), black), the intensity of peak decreases in the simulated spectrum for Model 2 (Figure 4(B), red). Such change agrees well with that observed in the experimental data (Figure 2(B)). Specifically, in this model, the central Ce atom was shifted along the [010] direction so that the distance of the 4 short Ce-O bonds is 2.22 Å, the same as that obtained using differential QEXAFS analysis.[14] Because the agreement between the simulated and experimental trends is qualitative, we cannot discriminate between the two models. It is possible that a combination of the two types of distortions (shifts of oxygen atoms in [111] direction and the shift of Ce atom in [010] cubic directions) is present. The theoretical spectrum corresponding to such a composite model is also shown in Fig. 4(B). We also checked the possibility that more distant neighbors to Ce can be distorted from their nominal Ce fluorite structure and such distortion may also affect the spectra. Theoretical modeling demonstrated no sensitivity to the changes in Ce-Ce distances (Figure S1 in Supplemental Material[23]), hence, our models that include only the changes in the nearest neighbor environment around active Ce units are validated. Based on these results, we conclude that the electroactive species in CGO could take the distorted structure of M1 and/or M2 due to the existence of a small population of oxygen vacancies introduced by Gd dopants. When the external electric field is applied, those distorted structures become more ordered (as indicated by the increase of the second peak in Figure 2(B) and 4(B) and our previous results[14]). Changing from distorted to ordered structures, the displacement of atoms induces large mechanical response of CGO materials.

To summarize, the combination of in situ high energy resolution XAS measurements aided by their theoretical modeling presents a powerful tool for local structural analysis. It sheds light on the local structural distortions in CGO that exist around Ce atoms, located near an oxygen vacancy, and the modification of these active units by external electric fields. The unique advantage of the HERFD method used in this work is in its ability to uncover the geometric nature of a small number of active local units whose atomic distortions change under application of electric fields. Specifically, in the initial equilibrium ("field-off") state, the small population of Ce-7O-1O_v units deviate locally from the cubic symmetry, producing a range of the Ce-O bonds, which are, on average, shorter than those in the Ce-8O units that contain no vacancy. These local deviations from the fluorite structure result from uncorrelated displacements of Ce and O atoms within the Ce-7O-1O_v units. Application of the electric field results in the reversal of the distortions towards the more symmetric (cubic) environment around Ce. We identified two plausible geometric models of local distortions in the Ce-7O-1O_v units that show good agreement with the experimental HERFD spectra and are quantitatively validated by the previous findings of differential EXAFS, XANES and macroscopic strain studies, all of which were limited by providing only the average magnitude of the displacements but not the directions. This knowledge of the nature of local distortions in Gd-doped ceria gives access to this important structural descriptor of macroscopic electromechanical properties in general and non-classical electrostriction in particular.

ACKNOWLEDGEMENTS

We acknowledge funding of this work by the Division of Chemical Sciences, Geosciences, and Biosciences within the U. S. Department of Energy Office of Basic Energy Sciences, Grant No. DE-FG02-03ER15476. A.I.F. is the Weston Visiting Professor at the Weizmann Institute of Science. We are grateful to K. Kvashnina and P. Glatzel for providing Ge crystals for the Ce L_3 HERFD measurements at the Beamline BL6-2 at the SSRL. O.K. and I.L gratefully acknowledge the assistance of the Nancy and Stephen Grand Research Center for Sensors and Security.

[1] S.-E. Park and T. R. Shrout, "Characteristics of relaxor-based piezoelectric single crystals for ultrasonic transducers," IEEE Trans. Ultrason., Ferroelect., Freq. Control **44**(5), 1140 (1997).

[2] F. Carpi, S. Bauer, and D. De Rossi, "Stretching Dielectric Elastomer Performance," Science **330**(6012), 1759 (2010).

[3] C. Keplinger, J.-Y. Sun, C. C. Foo, P. Rothemund, G. M. Whitesides, and Z. Suo, "Stretchable, Transparent, Ionic Conductors," Science **341**(6149), 984 (2013).

[4] D. Damjanovic, A. Biancoli, L. Batooli, A. Vahabzadeh, and J. Trodahl, "Elastic, dielectric, and piezoelectric anomalies and Raman spectroscopy of $0.5Ba(Ti_{0.8}Zr_{0.2})O_3 - 0.5(Ba_{0.7}Ca_{0.3})TiO_3$," Appl. Phys. Lett. **100**(19), 192907 (2012).

[5] R. Korobko, A. Patlolla, A. Kossoy, E. Wachtel, H. L. Tuller, A. I. Frenkel, and I. Lubomirsky, "Giant Electrostriction in Gd-Doped Ceria," Adv. Mater. **24**(43), 5857 (2012).

[6] R. J. Zednik, A. Varatharajan, M. Oliver, N. Valanoor, and P. C. McIntyre, "Mobile Ferroelastic Domain Walls in Nanocrystalline PZT Films: the Direct Piezoelectric Effect," Adv. Funct. Mater. **21**(16), 3104 (2011).

[7] Z. Kighelman, D. Damjanovic, M. Cantoni, and N. Setter, "Properties of ferroelectric $PbTiO_3$ thin films," J. Appl. Phys. **91**(3), 1495 (2002).

[8] Q. M. Zhang, H. Li, M. Poh, F. Xia, Z. Y. Cheng, H. Xu, and C. Huang, "An all-organic composite actuator material with a high dielectric constant," Nature **419**(6904), 284 (2002).

[9] Q. M. Zhang, V. Bharti, and X. Zhao, "Giant Electrostriction and Relaxor Ferroelectric Behavior in Electron-Irradiated Poly(vinylidene fluoride-trifluoroethylene) Copolymer," Science **280**(5372), 2101 (1998).

[10] K. M. Ok, E. O. Chi, and P. S. Halasyamani, "Bulk characterization methods for non-centrosymmetric materials: Second-harmonic generation, piezoelectricity, pyroelectricity, and ferroelectricity," Chem. Soc. Rev. **35**(8), 710 (2006).

[11] Z. L. Wang, X. Y. Kong, Y. Ding, P. Gao, W. L. Hughes, R. Yang, and Y. Zhang, "Semiconducting and Piezoelectric Oxide Nanostructures Induced by Polar Surfaces," Adv. Funct. Mater. **14**(10), 943 (2004).

[12] R. E. Newnham, V. Sundar, R. Yimnirun, J. Su, and Q. M. Zhang, "Electrostriction: Nonlinear Electromechanical Coupling in Solid Dielectrics," J. Phys. Chem. B **101**(48), 10141 (1997).

[13] N. Yavo, A. D. Smith, O. Yeheskel, S. Cohen, R. Korobko, E. Wachtel, P. R. Slater, and I. Lubomirsky, "Large Nonclassical Electrostriction in (Y, Nb)-Stabilized δ-Bi_2O_3," Adv. Funct. Mater. **26**(7), 1138 (2016).

[14] R. Korobko, A. Lerner, Y. Li, E. Wachtel, A. I. Frenkel, and I. Lubomirsky, "In-situ extended X-ray absorption fine structure study of electrostriction in Gd doped ceria," Appl. Phys. Lett. **106**(4), 042904 (2015).

[15] K. Hämäläinen, D. P. Siddons, J. B. Hastings, and L. E. Berman, "Elimination of the inner-shell lifetime broadening in x-ray-absorption spectroscopy," Phys. Rev. Lett. **67**(20), 2850 (1991).

[16] *EXAFS Spectroscopy*, edited by B. K. Teo and D. C. Joy (Plenum, New York, 1981).

[17] J. Sa, J. Szlachetko, M. Sikora, M. Kavcic, O. V. Safonova, and M. Nachtegaal, "Magnetic manipulation of molecules on a non-magnetic catalytic surface," Nanoscale **5**(18), 8462 (2013).

[18] G. Smolentsev, A. A. Guda, M. Janousch, C. Frieh, G. Jud, F. Zamponi, M. Chavarot-Kerlidou, V. Artero, J. A. van Bokhoven, and M. Nachtegaal, "X-ray absorption spectroscopy with time-tagged photon counting: application to study the structure of a Co(I) intermediate of H_2 evolving photo-catalyst," Faraday Discussions **171**, 259 (2014).

[19] J. Szlachetko, J. Sá, M. Nachtegaal, U. Hartfelder, J.-C. Dousse, J. Hoszowska, D. L. Abreu Fernandes, H. Shi, and C. Stampfl, "Real Time Determination of the Electronic Structure of Unstable Reaction Intermediates during Au_2O_3 Reduction," J. Phys. Chem. Lett. **5**(1), 80 (2014).

[20] C. Paun, O. V. Safonova, J. Szlachetko, P. M. Abdala, M. Nachtegaal, J. Sa, E. Kleymenov, A. Cervellino, F. Krumeich, and J. A. van Bokhoven, "Polyhedral CeO_2 Nanoparticles: Size-Dependent Geometrical and Electronic Structure," J. Phys. Chem. C **116**(13), 7312 (2012).

[21] K. O. Kvashnina, S. M. Butorin, and P. Glatzel, "Direct study of the f-electron configuration in lanthanide systems," J. Anal. At. Spectrom. **26**(6), 1265 (2011).

[22] D. Sokaras, T.-C. Weng, D. Nordlund, R. Alonso-Mori, P. Velikov, D. Wenger, A. Garachtchenko, M. George, V. Borzenets, B. Johnson, T. Rabedeau, and U. Bergmann, "A seven-crystal Johann-type hard x-ray spectrometer at the Stanford Synchrotron Radiation Lightsource," Rev. Sci. Instrum. **84**(5), 053102 (2013).

[23] See supplementary material at http://dx.doi.org/10.1063/1.4952645 for the details of the HERFD measurements, the estimate of the molar fraction of active species, and the details of FEFF9 modeling..

[24] A. Kossoy, Q. Wang, R. Korobko, V. Grover, Y. Feldman, E. Wachtel, A. K. Tyagi, A. I. Frenkel, and I. Lubomirsky, "Evolution of the local structure at the phase transition in $CeO_2 - Gd_2O_3$ solid solutions," Phys. Rev. B **87**(5), 054101 (2013).

[25] A. Kotani, K. O. Kvashnina, S. M. Butorin, and P. Glatzel, "A new method of directly determining the core–hole effect in the Ce L_3 XAS of mixed valence Ce compounds—An application of resonant X-ray emission spectroscopy," J. Electron Spectrosc. Relat. Phenom. **184**(3–6), 210 (2011).

[26] A. V. Soldatov, T. S. Ivanchenko, S. Della Longa, A. Kotani, Y. Iwamoto, and A. Bianconi, "Crystal-structure effects in the Ce L_3-edge x-ray-absorption spectrum of CeO_2: Multiple-scattering resonances and many-body final states," Phys. Rev. B **50**(8), 5074 (1994).

[27] T.-S. Wu, Y. Zhou, R. F. Sabirianov, W.-N. Mei, Y.-L. Soo, and C. L. Cheung, "X-ray absorption study of ceria nanorods promoting the disproportionation of hydrogen peroxide," Chem. Commun. **52**(28), 5003 (2016).

[28] H. Dexpert, R. C. Karnatak, J. M. Esteva, J. P. Connerade, M. Gasgnier, P. E. Caro, and L. Albert, "X-ray absorption studies of CeO_2, PrO_2, and TbO_2. II. Rare-earth valence state by L_{III} absorption edges," Phys. Rev. B **36**(3), 1750 (1987).

[29] J. J. Rehr, J. J. Kas, M. P. Prange, A. P. Sorini, Y. Takimoto, and F. Vila, "Ab initio theory and calculations of X-ray spectra," Comptes Rendus Physique **10**(6), 548 (2009).

[30] J. J. Rehr, J. J. Kas, F. D. Vila, M. P. Prange, and K. Jorissen, "Parameter-free calculations of X-ray spectra with FEFF9," Phys. Chem. Chem, Phys. **12**(21), 5503 (2010).

[31] J. J. Rehr and R. C. Albers, "Theoretical approaches to x-ray absorption fine structure," Rev. Mod. Phys. **72**(3), 621 (2000).

[32] A. Kotani, K. O. Kvashnina, S. M. Butorin, and P. Glatzel, "Spectator and participator processes in the resonant photon-in and photon-out spectra at the Ce L_3 edge of CeO_2," Eur. Phys. J. B **85**(8), 257 (2012).